

Imaging with neutral atoms—a new matter-wave microscope

M. KOCH^{*}, S. REHBEIN[†], G. SCHMAHL[‡], T. REISINGER^{*},
G. BRACCO[§], W. E. ERNST^{*} & B. HOLST^{*#}

^{*}Graz University of Technology, Institute of Experimental Physics, Petersgasse 16, 8010 Graz,
Austria

[†]BESSY m.b.H., Albert-Einstein-Strasse 15, 12489 Berlin, Germany

[‡]University of Göttingen, Institute for X-ray Physics, Friedrich-Hund-Platz 1, 37077 Göttingen,
Germany

[§]University of Genova, Department of Physics and CNR-IMEM, V. Dodecanesco 33, 16146 Genova,
Italy

[#]Present address: Department of Physics and Technology, University of Bergen, Allegaten 55, 5007
Bergen, Norway

Key words. Atom optics, matter-wave, microscopy, micro-skimmer, zone plate.

Summary

Matter-wave microscopy can be dated back to 1932 when Max Knoll and Ernst Ruska published the first image obtained with a beam of focussed electrons. In this paper a new step in the development of matter-wave microscopy is presented. We have created an instrument where a focussed beam of neutral, ground-state atoms (helium) is used to image a sample. We present the first 2D images obtained using this new technique. The imaged sample is a free-standing hexagonal copper grating (with a period of about 36 μm and rod thickness of about 8 μm). The images were obtained in transmission mode by scanning the focussed beam, which had a minimum spot size of about 2.0 μm in diameter (full width at half maximum) across the sample. The smallest focus achieved was $1.9 \pm 0.1 \mu\text{m}$. The resolution for this experiment was limited by the speed ratio of the atomic beam through the chromatic aberrations of the zone plate that was used to focus. Ultimately the theoretical resolution limit is set by the wavelength of the probing particle. In praxis, the resolution is limited by the source and the focussing optics.

Introduction

Microscopes are vital tools in almost all branches of science. They can be separated into three major groups: (i) optical microscopes, based on electromagnetic radiation; (ii) scanning probe microscopes such as scanning tunnelling microscopes (STM) or atomic force microscopes (AFM) and, (iii) matter-wave microscopes, at present almost exclusively electron microscopes, where massive particles are used as the imaging probe.

The importance of optical microscopes throughout the centuries can hardly be overstated and it is often said that the field of nanotechnology was born with the invention of the STM in the early 1980s (Binnig *et al.*, 1982). Matter-wave microscopy dates back to 1932 when Max Knoll and Ernst Ruska published an image obtained with a beam of focussed electrons (Knoll & Ruska, 1932). To this day electron microscopes of various types remain extremely important experimental tools in many branches of science.

In this paper we present a new matter-wave microscope that uses neutral ground-state atoms (helium) to image a sample. Helium atom scattering is already a well-established technique for investigating the structural and dynamic properties of surfaces (Farias & Rieder, 1998). Helium atom microscopy offers two major advantages: First, the probing helium atoms have very low energy, typically 20–100 meV for a de Broglie wavelength of 1–0.4 Å compared to hundreds of eV for electrons of comparable wavelengths. Second, the atoms are uncharged and chemically inert. This means that fragile samples can be investigated without damage, insulating materials can be investigated with no need for a conducting coating, and samples with high aspect ratios can be investigated. The focussing also opens the scope for carrying out diffraction studies on micro-crystallites. In that context, samples such as two-dimensional protein crystals, that is, porins, are very promising.

A range of experiments has focussed atoms and molecules using magnetic or optical fields (Reuss, 1988). However, these techniques are not applicable for the helium atoms (⁴He) used in the matter-wave microscope presented here because of their weak polarizability and lack of spin. Thus the only means of focussing are via the wave properties of the atom, with the additional limitation that helium atoms at meV energies do not

normally penetrate solid matter. This means that only mirrors or diffractive optical elements can be used. The latter consisting of free-standing structures that block selected portions of the wave front.

Neutral-atom focussing in one and two dimensions has been carried out using curved mirrors (Doak, 1992; Holst & Allison, 1997). So far the best focus achieved with this method was about 210 μm (Holst & Allison, 1997). Diffractive focussing has been demonstrated on two occasions using a Fresnel zone plate (Carnal *et al.*, 1991; Doak *et al.*, 1999). A Fresnel zone plate consists of a set of concentric rings blocking every other zone (Hecht, 2002).

The main result presented in this paper is the first real 2D image obtained using a focussed beam of neutral atoms (helium) to image a sample. The experiment was carried out using a new state-of-the-art Fresnel zone plate consisting of 2700 zones with an outer zone width of 50 nm.

Experimental set-up

Figure 1 (top panel) shows a light microscope image of the zone plate (centre disk with 540 μm diameter) used as atom optical element in the experiments presented here. A detailed description of the fabrication process can be found in literature (Rehbein, 2003). The zone plate is made of nickel and sits, slightly off centre, on an underlying Si membrane with a central hole. The support structure, also nickel, consisting of eight rings, is clearly visible. It can be seen that the central part of the zone plate (the first 240 zones) has been blocked by a circular stop. This is done to block the zeroth-order part of the diffracted beam as illustrated in the diagram in Fig. 2. The zone plate has 2700 zones with zone widths ranging from 165 nm at the outer rim of the circular stop to 50 nm of the outermost zones. The largest free-standing zone plate previously used had 670 zones (Doak *et al.*, 1999; Rehbein, 2001). Figure 1 (bottom panel) shows a scanning electron microscope (SEM) image of the outermost zones of 50 nm width. The thick crossbars (0.5 μm wide) crossing the picture left to right are radial support strips keeping the rings in place. The small gap between rings should be free from leftover resist. It is not possible to verify this explicitly since resist cannot be easily imaged with SEM. Also the width of the zones cannot be established exactly owing to possible field effects.

The experiments presented here were all carried out in a molecular beam apparatus named MaGiE, designed especially for microscopy experiments. A detailed description of the apparatus can be found in literature (Apfoltner, 2005). Figure 2 shows a diagram of the experimental set-up. A neutral, ground-state helium beam is created by a supersonic expansion from a 10- μm -diameter nozzle. Measurements were made at source pressure ranging from 10 to 190 bar. The nozzle temperature was kept at 320 K for all experiments, corresponding to an average beam velocity of 1865 m/s and a wavelength of 0.53 \AA . The average velocity, v , and speed ratio of the

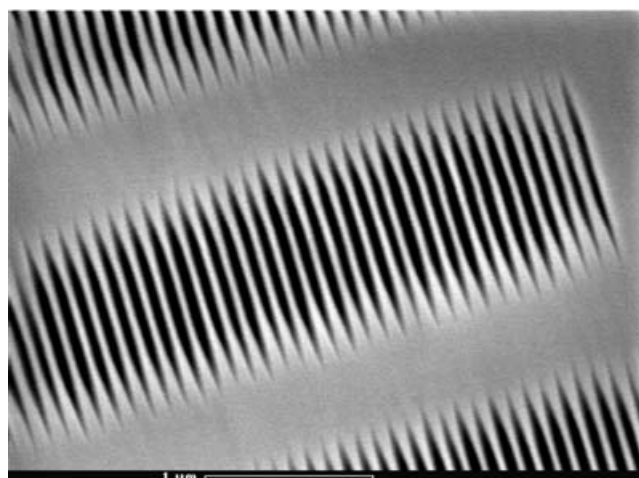
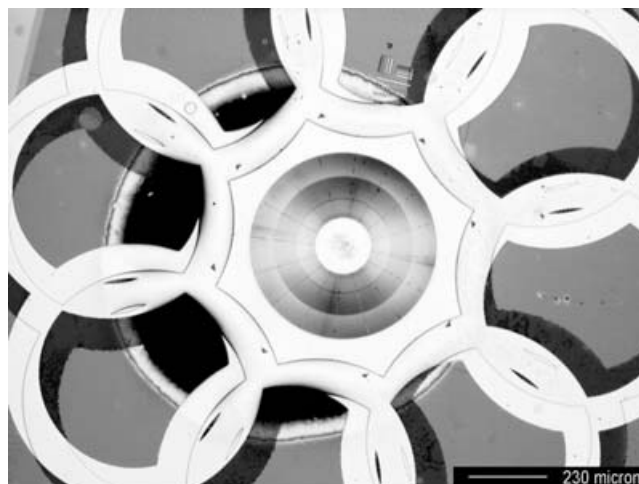


Fig. 1. Top panel: Light microscope image of the zone plate (central disk, slightly off centre) and its support structure (8 white rings). The zone plate and the support structure are made of nickel. In the middle of the zone plate a circular stop can be seen. This blocks the zero order part of the diffracted beam as illustrated in Fig. 2. Bottom panel: SEM image showing free standing outermost zones of 50 nm width which are held by radial support strips.

beam, S , were determined with time of flight (TOF) using a double-slit chopper (not shown in the diagram in Fig. 2). The speed ratio is defined as $S = 2\sqrt{\ln 2} v / \Delta v$ (Pauly, 2000) (where Δv is the full width at half maximum (FWHM) of the measured velocity distribution). The speed ratio varied from 16 ± 1 at 10-bar source pressure to 140 ± 3 at 190 bar, corresponding to a spread in wavelength of 0.06 \AA at 10 bar to 0.007 \AA at 190 bar. The central part of the supersonic expansion region was selected using a micro-skimmer. Two micro-skimmers ($2.4 \pm 0.2 \mu\text{m}$ and $1.2 \pm 0.1 \mu\text{m}$ in diameter) were used in the experiments presented here. The micro-skimmers were produced by pulling glass capillary tubes using a commercial puller (Braun *et al.*, 1997). The beam was focussed by the zone plate onto the image plane where the

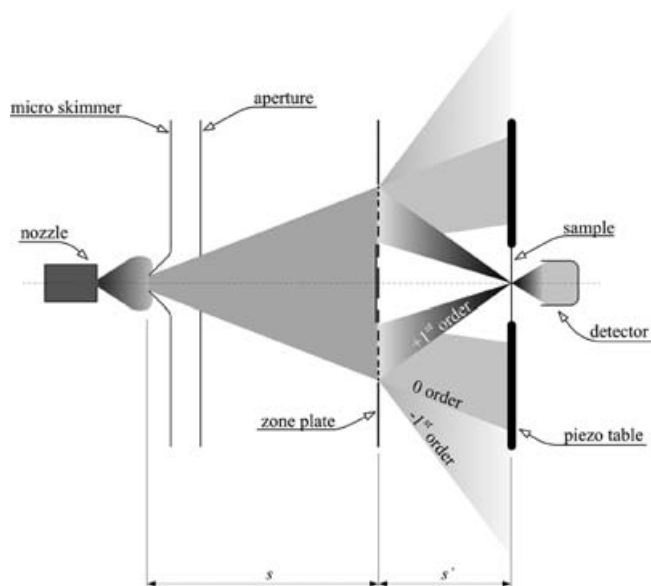


Fig. 2. Sketch of the scanning helium beam microscope. The source is given by a micro-skimmer and imaged by the zone plate's plus first diffraction order. In addition, the zero as well as the minus first order are indicated. s is the source to zone plate distance and s' the distance from zone plate to image plane. The sample can be scanned across the beam by a piezo table. The transmitted intensity of the beam is recorded at the back to obtain an image in transmission mode.

sample to be examined was located, mounted on a piezo table, which could be scanned in two dimensions with sub-micrometre resolution (Type PXY 100 SG-V from piezosystem jena GmbH). The transmitted part of the beam was detected using an electron bombardment detector mounted with a magnetic mass selector and a channeltron.

The zone plate was placed at the maximum possible distance $s = 1492$ mm from the source. The distance from the zone plate to the sample on the piezo table in front of the detector was variable in a range of 680 mm to 840 mm. In this way the distance s' from the zone plate to the sample could be optimized to place the sample in the image plane. Given the distribution of the rings on the zone plate and the wavelength of the beam, the expected focal length $f = 506$ mm could be calculated, giving an expected image distance of $s' = 765$ mm. Experimentally the optimum image position was found at $s' = 766 \pm 3$ mm by measuring the spot size at different distances to the zone plate as described in the next section.

Results and analysis

Figure 3 shows the first 2D images obtained using neutral atoms for imaging. The imaged sample is a free-standing hexagonal copper grating (36 μm period and 8 μm rod thickness). Using the 1.2- μm skimmer, the focussed atom-spot was about 3.0 μm in diameter for the upper image (obtained with a beam pressure of about 150 bar, signal 80 cts s^{-1} ,

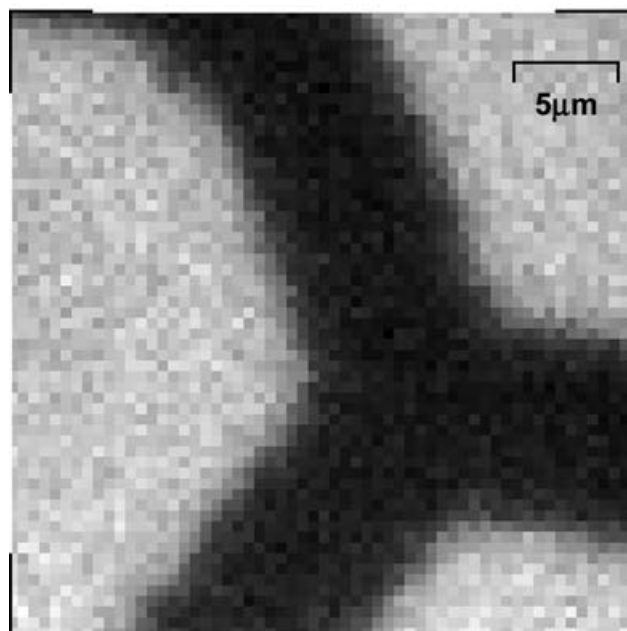
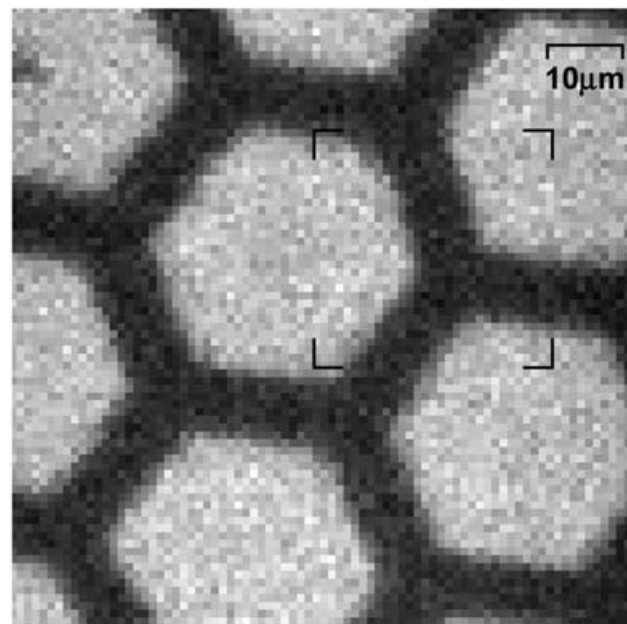


Fig. 3. The first 2D image obtained using neutral atoms (helium) to image a sample. The imaged sample is a hexagonal copper grating with a period of 36 μm and a rod thickness of 8 μm . The image is obtained in transmission mode by scanning the focussed beam across the sample (the sample is being moved). For the upper image the grating was scanned in 1- μm steps across a 3.0- μm -diameter beam spot, whereas for the lower image 0.5- μm steps and a 2.0- μm beam spot were used.

background 110 cts s^{-1}) and about 2.0 μm for the lower image (obtained with a beam pressure of about 180 bar, signal 70 cts s^{-1} , background 100 cts s^{-1}). For the first image the grating was scanned in 1- μm steps and for the second image in

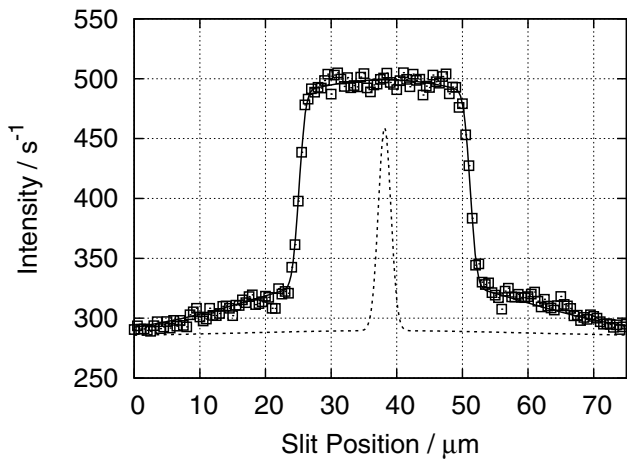


Fig. 4. Scan of a $25 \mu\text{m} \times 3 \text{mm}$ slit across the smallest obtained spot in steps of $1 \mu\text{m}$ with a measuring time of 30 s for each point. The actual detector signal is represented by squares and the solid line is a simulated scan across a Gaussian focus of $1.9 \pm 0.1 \mu\text{m}$ diameter (FWHM). The dashed line shows the reconstructed Gaussian spot (arbitrary Units).

0.5- μm steps. In order to obtain a suitable signal-to-noise ratio a measuring time for each pixel of 8 s for the upper image and 14 s for the lower image was necessary, giving a total recording time of about 14 h for each image. The temperature in the laboratory was kept stable to within 0.4 K during the entire measurement.

For a monochromatic beam the expected diameter of the focussed spot for the 1.2- μm skimmer is $0.62 \pm 0.05 \mu\text{m}$ (determined by the diameter of the skimmer and the geometrical configuration (s'/s)). To experimentally determine the spot size the sample was replaced with a vertical slit ($25 \mu\text{m} \times 3 \text{mm}$) and scanned horizontally in steps of $1 \mu\text{m}$ across the focussed spot. Figure 4 shows a scan across the smallest obtained spot at optimum distance to the zone plate. The squares represent the actual detector signal in counts per second. This spot was found to be $1.9 \pm 0.1 \mu\text{m}$ in diameter (FWHM; beam pressure 190 bar, measuring time for each point 30 s, signal 175cts s^{-1} and background 325cts s^{-1}). Since the slit was broader than the spot diameter, the intensity versus the slit position had a trapezoidal-like shape with the rising and the falling edge containing the information on the spot size. This information was extracted by fitting the data points with a mathematical model representing a slit scan across a Gaussian focus (solid line in Fig. 4): $\frac{1}{2}[\text{erf}(\frac{x-\mu+w/2}{\sigma\sqrt{2}}) - \text{erf}(\frac{x-\mu-w/2}{\sigma\sqrt{2}})]$, where μ and σ are the centre and the Gaussian standard deviation of the focus, respectively, w is the slit width and erf is the error function. The dashed line in Fig. 4 represents the reconstructed Gaussian spot (in arbitrary Units) based on the centre position and standard deviation obtained from the model above.

The velocity distribution of the beam induces a broadening of the focus through the chromatic aberrations of the zone

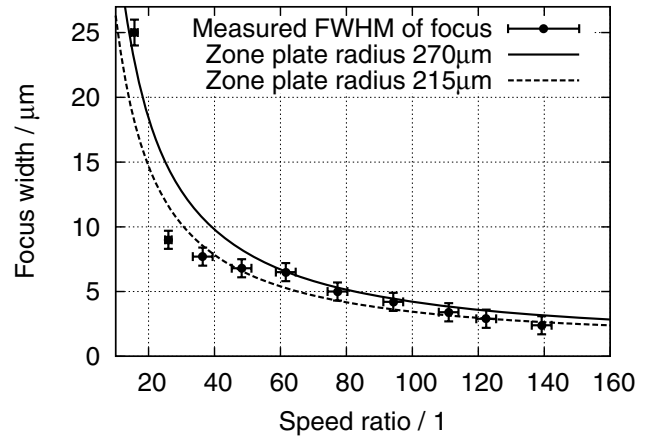


Fig. 5. Measured focussed spot-sizes (FWHM) from a micro-skimmer 2.4 ± 0.2 in diameter, using beams with speed ratios, S , ranging from 16 ± 1 to 140 ± 3 , corresponding to nozzle pressures, p_0 , from 10 to 190 bar. The lines show the theoretically predicted spot-sizes for two different zone plate diameters.

plate. To investigate this we carried out a series of experiments measuring the focussed spot size as a function of the speed ratio of the beam. Using a micro-skimmer of $2.4 \mu\text{m}$ diameter, the spot size was measured at the image position for speed ratios S in the range of 16 ± 1 to 140 ± 3 , realized with source pressures, p_0 , in the range of 10–190 bar. The results can be seen in Fig. 5. The two curves in the figure show the theoretically expected spot size for two different zone plate diameters. Basis is the formula for the transverse chromatic aberration, $\Delta\sigma_{\text{cm}}$, for a zone plate illuminated with polychromatic light from a pinhole, $\Delta\sigma_{\text{cm}} \approx r_N/R_m$ (Michette, 1986), where r_N is the radius of the zone plate and R_m is the resolving power $\lambda/\Delta\lambda$, which can be directly extracted from the speed ratio of the beam. The model used to calculate the curves takes into account the effect of the central circular obstruction on chromatic aberration (Michette, 1986). Furthermore, the model is adapted to our non-planewave set-up by taking the quadrature sum of the width due to aberration and the expected image width of the demagnified skimmer, assuming both contributions to be of Gaussian shape.

The upper curve shows the expected spot sizes using the nominal zone plate radius ($r_N = 270 \mu\text{m}$). The lower curve shows the expected spot sizes using an effective zone plate radius ($r_N = 215 \mu\text{m}$); estimated on the basis of the extension of the zeroth order (see Fig. 2), which could be clearly distinguished in the slit scans of the focussed spots. The fact that the extension of the zeroth order is smaller than expected from the nominal zone plate diameter indicates that a fraction of the outermost zones are in fact not free and that therefore the effective zone plate diameter is smaller than $540 \mu\text{m}$. This is supported by Fig. 5, where the curve corresponding to the estimated effective zone plate size provides the best fit to the experimental results.

It has previously been suggested (Doak *et al.*, 1999) that an additional broadening of the focussed beam could be caused by collisions in the beam in the funnel of the micro-skimmer, leading to an effective source size larger than the skimmer opening. For high pressures, the agreement with theory is excellent and we conclude that no broadening of the beam takes place through collisions of atoms in the skimmer funnel for the experiments presented here (one would expect such a broadening to increase with pressure). We note, however, that the experiments presented in Doak *et al.* (1999) while using a skimmer of similar size were carried out at flow rates up to about three times higher.

Conclusions and future work

In this paper we have presented the first 2D image obtained using a focussed beam of neutral atoms as an imaging probe. A zone plate with free-standing structures was used as focussing element. The resolving power was limited by the speed ratio of the beam in excellent agreement with the predicted chromatic aberrations for zone plates. No sign of broadening of the effective source size was observed.

We are currently working on improving the sampling rate and resolution of our microscope. This involves improving the sensitivity of the detector (DeKieviet *et al.*, 2000), the speed ratio of the beam, the mechanical stability of the apparatus, the thermal stability of the laboratory and continuing the development of atom optical elements, including focussing mirrors. The focussing mirrors remain a technical challenge, but they are promising because they do not suffer from chromatic aberrations and potentially have a higher reflectivity. Finally, they can be made with larger numerical apertures (the zone plates are limited by the width of the outermost zone).

Acknowledgements

We thank P. Pölt and E. Ingolić, FELMI-ZFE, Center for Electron Microscopy at Graz University of Technology, for assistance with the images in Fig. 1. This work was supported by the European Union FP6, program NEST - Adventure, contract no.

509014, project INA, and by the Austrian Science Foundation (FWF) project no. P17316-N02

References

- Farias, D. & Rieder, K.H. (1998) Atomic beam diffraction from solid surfaces. *Rep. Prog. Phys.* **61**, 1575–1664.
- Apfalter, A. (2005) Wiederaufbau und Test einer He-Streuapparat und erste Streuexperimente an amorpher sowie kristalliner SiO₂-Oberfläche. Master's thesis, Graz University of Technology, Institute of Experimental Physics.
- Binnig, G., Rohrer, H., Gerber, C., & Weibel, E. (1982) Surface studies by scanning tunneling microscopy. *Phys. Rev. Lett.* **49**, 57.
- Braun, J., Day, P.K., Toennies, J.P., Witte, G. & Neher, E. (1997) Micrometer-sized nozzles and skimmers for the production of supersonic He atom beams. *Rev. Sci. Instrum.* **68**(8), 3001–3009.
- Carnal, O., Sigel, M., Sleator, T., Takuma, H. & Mlynek, J. (1991) Imaging and focusing of atoms by a Fresnel zone plate. *Phys. Rev. Lett.* **67**(23), 3231–3234.
- DeKieviet, M., Dubbers, D., Klein, M., Piele, U. & Schmidt, C. (2000) Design and performance of a highly efficient mass spectrometer for molecular beams. *Rev. Sci. Instrum.* **71**(5), 2015–2018.
- Doak, R.B. (1992) *Helium Atom Scattering from Surfaces* (ed. by E. Hulpke), pp. 5–24. Springer-Verlag, Berlin.
- Doak, R.B., Grisenti, R.E., Rehbein, S., Schmahl, G., Toennies, J.P. & Wöll, C. (1999) Towards realization of an atomic de Broglie microscope: helium atom focusing using Fresnel zone plates. *Phys. Rev. Lett.* **83**(21), 4229–4232.
- Hecht, E. (2002) *Optics*. Addison Wesley, New York.
- Holst, B. & Allison, W. (1997) An atom-focusing mirror. *Nature* **390**, 244.
- Knoll, M. & Ruska, E. (1932) Das Elektronenmikroskop. *Z. Physik* **78**, 318.
- Michette, A.G. (1986) *Optical Systems for Soft X Rays*. Plenum Press, New York.
- Pauly, H. (2000) *Atom, Molecule and Cluster Beams I*. Springer-Verlag, Berlin.
- Rehbein, S. (2001) Entwicklung von freitragenden Zonenplatten zur Fokussierung und Monochromatisierung thermischer Helium-Atomstrahlen. Ph.D. Thesis, University of Göttingen, Institute for X-ray Physics.
- Rehbein, S. (2003) Nanofabrication of diffractive optics for soft x-ray and atom beam focusing. *J. Phys. IV France* **104**, 207–210.
- Reuss, J. (1988) State selection by nonoptical methods. *Atomic and Molecular Beam Methods* (ed. by G. Scoles), Volume 1, pp. 277–292. Oxford University Press.